Hybrid Position/Force Control of Two Cooperative Flexible Manipulators Working in 3D Space

Mitsuhiro Yamano, Jin-Soo Kim and Masaru Uchiyama
Department of Aeronautics and Space Engineering, Tohoku University
Aramaki-aza-Aoba, Aoba-ku, Sendai 980-77, Japan

Abstract

In this paper, we discuss the control scheme on cooperative control of two flexible manipulators handling a rigid object in 3D space. We propose a control scheme which consists of hybrid position/force control and vibration suppression control. Hybrid position/force control is extended from that for two cooperative rigid manipulators to that for flexible ones. In addition to the control, vibration suppression control based upon the dynamics of both the flexible manipulators and the object is applied. To illustrate the validity of the proposed control scheme, we show experimental results.

1 Introduction

Recent developments in space technology demand effective control laws for space manipulators. A space manipulator must be of very light-weight so that a rocket or a shuttle can carry it. But long and light-weight links don't have enough rigidity. This lack of rigidity causes vibrations of the links.

Many studies have been done on single-arm flexible manipulators [1]–[8]. But the tasks, such as transporting a long and heavy object and assembling parts, are carried out more efficiently and dexterously by multiple arms. However, the effective cooperative control schemes for such advanced tasks in 3D space have been studied for only rigid manipulators [9]–[12]. Recently, some researches on cooperative control schemes of planar flexible manipulators have been reported [13]–[15]. The planar manipulators, however, cannot be employed for complex tasks in 3D space, and therefore, it is needed to deal with cooperative tasks by multi-link flexible manipulators working in 3D space. For this reason, we have started the study of two cooperative flexible manipulators and proposed the control scheme to handle a light-weight and rigid object in 3D space [16].

In this paper, we present the control scheme to handle a heavy rigid object in 3D space. As we consider the mass of the object in the control scheme, a heavy object can be handled. We first summarize the task vectors of forces, velocities and positions and present the kinematic, static and dynamic equations of the cooperative flexible manipulators including the object. And then we propose the control scheme consisting of hybrid position/force control based on the kinematics and the statics and vibration suppression control based on the dynamics. Finally, we show experimental results to illustrate the validity of the proposed control scheme.

2 Kinematics, Statics and Dynamics

The controller being proposed in this paper is based on the kinematic, static and dynamic equations of two cooperative manipulators and the object forming a closed kinematic chain.

In this section, the kinematic and static equations are derived by using the kinematics of a single-arm flexible manipulator and the task vectors proposed in [10], and the dynamic equations are presented.

In the following paragraphs, subscript n (=1, 2) represents the arm number.

2.1 Kinematics of a single-arm flexible manipulator

The positions and orientations of a flexible manipulator's hand are calculated from the joint angles $\boldsymbol{\theta}_n$ and elastic deflections of the links $\boldsymbol{e}_n$. Therefore, translational and angular velocities $\boldsymbol{s}_{hn}$ are calculated by

$$ {}^{0}\boldsymbol{s}_{hn} = \boldsymbol{J}_{hn}\dot{\boldsymbol{q}}_n, \tag{1}$$

where

$$\boldsymbol{J}_{hn} = \left[\begin{array}{cc} \boldsymbol{B}_s \dfrac{\partial \boldsymbol{p}_{hn}}{\partial \boldsymbol{\theta}_n} & \boldsymbol{B}_s \dfrac{\partial \boldsymbol{p}_{hn}}{\partial \boldsymbol{e}_n} \end{array} \right], \tag{2}$$

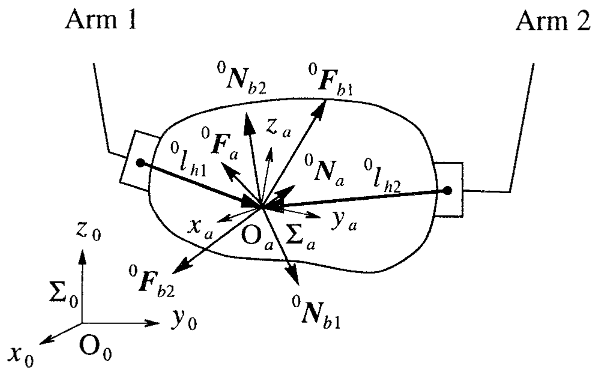

Figure 1: Two arms holding a single object.

$$q_n = \left[\ \theta_n^T \quad e_n^T \ \right]^T, \tag{3}$$

$$B_s = \mathrm{diag}\left[\ E_3, \quad B_0 \ \right], \tag{4}$$

p_{hn} represents positions/orientations of each hand, E_3 is a 3×3 unit matrix and B_0 is a 3×3 matrix that transforms the time derivatives of angles to the angular velocities.

2.2 Task vectors

To describe the kinematics and the statics of the two cooperative arms forming a closed kinematic chain, we use the task vectors of generalized forces, velocities and positions [10].

Let us consider two arms holding an object as shown in Figure 1. Σ_0 represents the base coordinate system. The coordinate system Σ_a is fixed to the object and a virtual stick $^0l_{hn}$ is fixed to each hand. Here, we suppose that the deformation of the object and the slips of the hands against the object are very small. Let us denote the forces/moments at the tip of the virtual sticks as

$$^0f_{bn} = \left[\ ^0F_{bn}^T \quad ^0N_{bn}^T \ \right]^T. \tag{5}$$

The relation between $^0f_{bn}$ and the external forces/moments ^0f_a is written as follows:

$$^0f_a = {}^0f_{b1} + {}^0f_{b2}. \tag{6}$$

Using the matrix pseudoinverse technique, the internal forces/moments ^0f_r are calculated as follows [10]:

$$^0f_r = \frac{1}{2}\left(^0f_{b1} - {}^0f_{b2} \right). \tag{7}$$

Using the concept of virtual work, the solutions of the velocities and the positions corresponding to ^0f_a and ^0f_r are, respectively, given by

$$^0s_a = \frac{1}{2}\left(^0s_{b1} + {}^0s_{b2} \right), \tag{8}$$

$$^0\Delta s_r = {}^0s_{b1} - {}^0s_{b2}, \tag{9}$$

$$^0p_a = \frac{1}{2}\left(^0p_{b1} + {}^0p_{b2} \right), \tag{10}$$

$$^0\Delta p_r = {}^0p_{b1} - {}^0p_{b2}, \tag{11}$$

where $^0s_{bn}$ and $^0p_{bn}$, respectively, represent the velocities and the positions corresponding to $^0f_{bn}$. We define the task vectors of generalized forces, generalized velocities and generalized positions as

$$\eta = \left[\ ^0f_a^T \quad ^af_r^T \ \right]^T, \tag{12}$$

$$u = \left[\ ^0s_a^T \quad ^a\Delta s_r^T \ \right]^T, \tag{13}$$

$$z = \left[\ ^0p_a^T \quad ^a\Delta p_r^T \ \right]^T. \tag{14}$$

2.3 Jacobian matrix for the closed kinematic chain

From the kinematics of a single-arm flexible manipulator and the task vectors, we derive the kinematics and statics of two cooperative flexible manipulators forming a closed kinematic chain. The kinematics and the statics are described by using Jacobian matrix for the manipulators.

Let us denote the joint torques, joint angles and the link deflections of the dual arms as

$$\tau = \left[\ \tau_1^T \quad \tau_2^T \ \right]^T, \tag{15}$$

$$\theta = \left[\ \theta_1^T \quad \theta_2^T \ \right]^T, \tag{16}$$

$$e = \left[\ e_1^T \quad e_2^T \ \right]^T, \tag{17}$$

$$q = \left[\ \theta^T \quad e^T \ \right]^T. \tag{18}$$

As each virtual stick is fixed to each hand, s_{bn} is calculated from q_n and $\dot{q}_{hn}$ by using the same technique as Equation (1). Therefore, from Equations (8), (9) and (13), the relation between u and $\dot{q}$ is written as follows [16]:

$$\begin{aligned} u &= J_\theta(q)\,\dot{\theta} + J_e(q)\,\dot{e} \\ &= J(q)\,\dot{q}, \end{aligned} \tag{19}$$

where J_θ and J_e is, respectively, Jacobian matrix with respect to θ and e, and J is Jacobian matrix with respect to q.

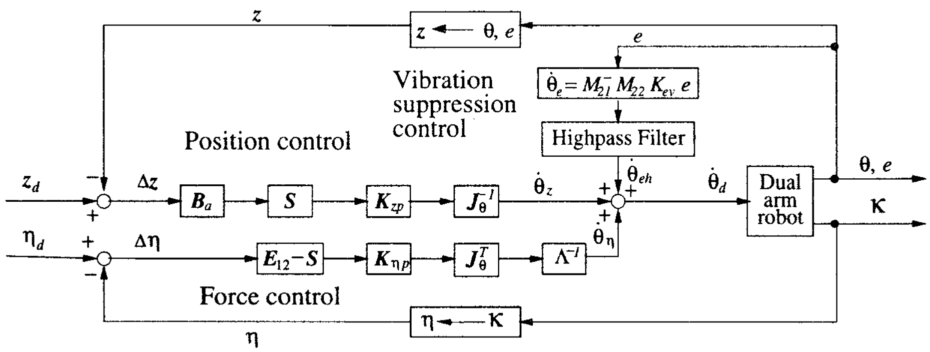

Figure 2: Hybrid position/force and vibration suppression controller.

Considering Equation (19) and virtual work, the joint torques to be balanced with generalized forces are obtained by

$$\boldsymbol{\tau}_\eta = \boldsymbol{J}_\theta^T \boldsymbol{\eta}. \tag{20}$$

2.4 Dynamics

To establish a vibration suppression control, we use the dynamic equations of two cooperative flexible manipulators forming a closed kinematic chain. The equations are formulated from the dynamic equations of a single-arm flexible manipulator and the object, and constrained conditions [15]. The equations can be written as follows:

$$\begin{aligned}\boldsymbol{\tau} &= \boldsymbol{M}_{11}(\boldsymbol{q})\ddot{\boldsymbol{\theta}} + \boldsymbol{M}_{12}(\boldsymbol{q})\ddot{e} + \boldsymbol{h}_1(\boldsymbol{q}, \dot{\boldsymbol{q}}) \\ &+ \boldsymbol{g}_1(\boldsymbol{q}) + \boldsymbol{J}_{\theta r}^T(\boldsymbol{q})\,{}^a\boldsymbol{f}_r,\end{aligned} \tag{21}$$

$$\begin{aligned}\boldsymbol{0} &= \boldsymbol{M}_{21}(\boldsymbol{q})\ddot{\boldsymbol{\theta}} + \boldsymbol{M}_{22}(\boldsymbol{q})\ddot{e} + \boldsymbol{h}_2(\boldsymbol{q}, \dot{\boldsymbol{q}}) \\ &+ \boldsymbol{K}_{22}\boldsymbol{e} + \boldsymbol{g}_2(\boldsymbol{q}) + \boldsymbol{J}_{er}^T(\boldsymbol{q})\,{}^a\boldsymbol{f}_r,\end{aligned} \tag{22}$$

where $\boldsymbol{M}_{ij}$ represents an inertia matrix ($i,\ j = 1,\ 2$), $\boldsymbol{h}_1$ and $\boldsymbol{h}_2$ represent centrifugal and Corioli's force vectors, $\boldsymbol{K}_{22}$ represents a stiffness matrix, $\boldsymbol{g}_1$ and $\boldsymbol{g}_2$ represent gravity vectors corresponding to joint motions and link deflections respectively, and $\boldsymbol{J}_{\theta r}$ and $\boldsymbol{J}_{er}$ represent Jacobian matrix of ${}^a\Delta\boldsymbol{s}_r$ with respect to $\boldsymbol{\theta}$ and $\boldsymbol{e}$ respectively.

3 Control Scheme

The block diagram of hybrid position/force control and vibration suppression control schemes is shown in Figure 2. Hybrid position/force control is based upon the kinematics and statics of two cooperative flexible manipulators, while vibration suppression control is based upon the dynamics of both the manipulators and the object. We establish the control scheme for the manipulators whose motors are driven by velocity hardware servo. The velocity commands are calculated from position control, force control and vibration suppression control as follows:

$$\dot{\boldsymbol{\theta}}_d = \dot{\boldsymbol{\theta}}_z + \dot{\boldsymbol{\theta}}_\eta + \dot{\boldsymbol{\theta}}_{eh}. \tag{23}$$

To control the positions of the object, absolute positions ${}^0\boldsymbol{p}_a$ are controlled by using the Jacobian matrix $\boldsymbol{J}_\theta$ defined by Equation (19). Assuming that $\dot{\boldsymbol{e}}$ are kept small by vibration suppression control, $\boldsymbol{J}_e\dot{\boldsymbol{e}}$ can be neglected. Therefore, $\dot{\boldsymbol{\theta}}_z$ is calculated as follows:

$$\dot{\boldsymbol{\theta}}_z = \boldsymbol{J}_\theta^{-1}\boldsymbol{S}\boldsymbol{K}_{zp}\boldsymbol{B}_a(\boldsymbol{z}_d - \boldsymbol{z}), \tag{24}$$

where

$$\boldsymbol{B}_a = \mathrm{diag}\left[\ \boldsymbol{B}_s,\quad \boldsymbol{E}_6\ \right], \tag{25}$$

$$\boldsymbol{S} = \mathrm{diag}\left[\ \boldsymbol{E}_6,\quad \boldsymbol{0}\ \right], \tag{26}$$

$\boldsymbol{z}_d$, $\boldsymbol{z}$, respectively, represent the desired and current generalized positions. $\boldsymbol{S}$ is a selective matrix that selects ${}^0\boldsymbol{p}_a$ from $\boldsymbol{z}$.

To control forces exerted on the object, the internal forces and the relation between the joint torques and velocity commands are considered. As the motor drivers include velocity hardware servo, the relation between the joint torques and velocity commands $\dot{\boldsymbol{\theta}}_d$ is, approximately, assumed as

$$\boldsymbol{\tau} = \boldsymbol{\Lambda}(\dot{\boldsymbol{\theta}}_d - \dot{\boldsymbol{\theta}}). \tag{27}$$

Force control low is based upon the relation between joint torques and internal forces in the stationary condition (i.e., $\dot{\boldsymbol{\theta}} = \dot{\boldsymbol{\theta}}_z = \dot{\boldsymbol{\theta}}_{eh} = \boldsymbol{0}$ and $\boldsymbol{\tau} = \boldsymbol{\tau}_\eta$), and $\dot{\boldsymbol{\theta}}_\eta$ is computed as

$$\dot{\boldsymbol{\theta}}_\eta = \boldsymbol{\Lambda}^{-1}\boldsymbol{J}_\theta^T(\boldsymbol{E}_{12} - \boldsymbol{S})\boldsymbol{K}_{\eta p}(\boldsymbol{\eta}_d - \boldsymbol{\eta}), \qquad (28)$$

where $\boldsymbol{\eta}_d$ and $\boldsymbol{\eta}$, respectively, represent desired and current generalized forces and $\boldsymbol{K}_{\eta p}$ is a gain matrix. $\boldsymbol{\eta}$ is calculated from $\boldsymbol{\kappa}$ to represent forces/moments measured by the force/torque sensors.

Vibration suppression control is based upon Equation (22). If

$$\text{rank}\boldsymbol{M}_{21} = \dim(\boldsymbol{e}), \qquad (29)$$

and the joint accelerations are given by

$$\ddot{\boldsymbol{\theta}} = -\boldsymbol{M}_{21}^{-}\boldsymbol{M}_{22}\boldsymbol{K}_{ev}\Delta\dot{\boldsymbol{e}}, \qquad (30)$$

where $\boldsymbol{M}_{21}^{-}$ is generalized inverse of $\boldsymbol{M}_{21}$,

$$\Delta\boldsymbol{e} = \boldsymbol{e}_0 - \boldsymbol{e}, \qquad (31)$$

$$\boldsymbol{e}_0 = -\boldsymbol{K}_{22}^{-1}\left(\boldsymbol{g}_2 + \boldsymbol{J}_{re}^{T\,a}\boldsymbol{f}_r\right), \qquad (32)$$

then the following equations including a dumping term are obtained.

$$\Delta\ddot{\boldsymbol{e}} + \boldsymbol{K}_{ev}\Delta\dot{\boldsymbol{e}} + \boldsymbol{M}_{22}^{-1}\boldsymbol{K}_{22}\Delta\boldsymbol{e} = \boldsymbol{0}. \qquad (33)$$

To apply Equation (30) to the manipulators with velocity commanded motors and to reduce the calculations, $\dot{\boldsymbol{\theta}}_{eh}$ is calculated by using high-pass filter $\boldsymbol{S}_{high}$ [2] as

$$\dot{\boldsymbol{\theta}}_{eh} = \boldsymbol{S}_{high}\boldsymbol{M}_{21}^{-}\boldsymbol{M}_{22}\boldsymbol{K}_{ev}\,\boldsymbol{e}. \qquad (34)$$

4 Experiments

To show the effectiveness of the proposed control scheme, experiments on cooperative tasks are performed. The experimental manipulators handle a rigid object in 3D space.

4.1 Experimental setup

Figure 3 shows an overview of a dual-arm flexible manipulator named ADAM (Aerospace Dual-Arm Manipulator) [17]. ADAM has two arms and each arm has two flexible links and seven rotary joints. Figure 4 shows the joints, the motors and the links of Arm 2 and the deflections of a link. Table 1 shows the parameters of ADAM. The contact forces/moments at end-effectors are measured by using force/torque sensors while the link vibrations are measured by both strain gauges at the root of each link and the force/torque sensors. Assuming the moments of inertia of each elbow as zero, ϕ_{i3} $(i = x,\ y,\ z)$ of each arm depend δ_{ij} $(i = y,\ z;\ j = 3,\ 5)$ and ϕ_{i5} $(i = x,\ y,\ z)$ of the arm. Therefore, the link deflections $\boldsymbol{e}$ consists of δ_{ij} $(i = y,\ z;\ j = 3,\ 5)$ and ϕ_{i5} $(i = x,\ y,\ z)$ of the dual arms.

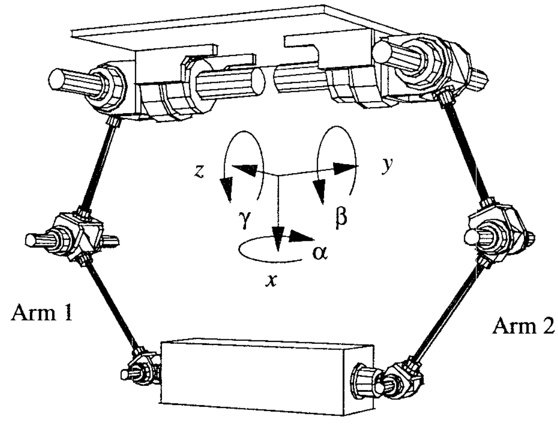

Figure 3: Overview of two cooperative flexible manipulator ADAM.

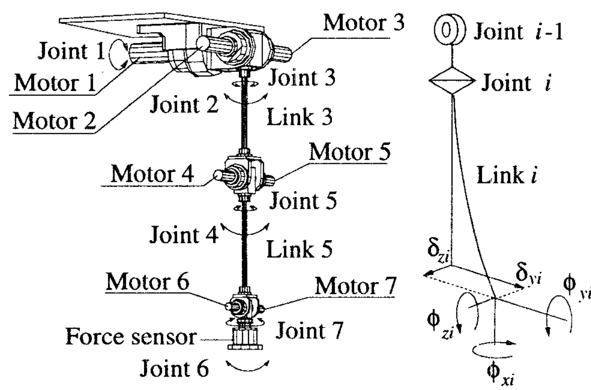

Figure 4: Joints, motors and links of Arm 2 and the deflections of a link (i=3, 5).

4.2 Experimental results

In the experiment, hybrid position/force control is realized by using all joints except joint 3 of each arm. Vibration suppression control is realized by using all joints. $\boldsymbol{K}_{zp} = 4.0\boldsymbol{E}_{12}$ [s^{-1}], $\boldsymbol{K}_{\eta p} = 0.3\boldsymbol{E}_{12}$, $\boldsymbol{K}_{ev} = 30\boldsymbol{E}_{14}$ [s^{-1}] and the cutoff frequency of the high-pass filter is 1 [Hz]. The desired positions/orientations are given by

$$\boldsymbol{z}_d(t) = \boldsymbol{z}(0) + (\boldsymbol{z}_g - \boldsymbol{z}(0))\left(t - \frac{\sin(\pi t)}{2\pi}\right), \qquad (35)$$

where $\boldsymbol{z}_g$ represents the goal of $\boldsymbol{z}$ and t represents time, and the desired forces/moments are constant.

The elastic deflections of the links are shown in Figure 5 and Figure 6, and reference and current values

Table 1: Parameters of ADAM and the object.

Parameter		Value
Length of link 3	[m]	0.50
Length of link 5	[m]	0.50
Bending stiffness of link 3	[Nm^2]	291.6
Bending stiffness of link 5	[Nm^2]	102.1
Torsional stiffness of link 3	[Nm^2]	224.3
Torsional stiffness of link 5	[Nm^2]	78.5
Mass of elbow	[kg]	6.0
Mass of wrist and end-effector	[kg]	2.7
Mass of object	[kg]	1.5

of the absolute positions/orientations and the internal forces/moments are shown in Figure 7 and Figure 8. As Figure 8 illustrates that internal forces are almost maintained, $\boldsymbol{e}_0$ is eliminated by the high-pass filter. Therefore, the vibrations are suppressed by vibration suppression control expressed by Equation (34) as illustrated in Figure 5 and Figure 6. As the vibration of the links are suppressed, it is valid to neglect $\boldsymbol{J}_e\dot{\boldsymbol{e}}$ in the position controller written by Equation (24). Therefore, current positions do not vibrate and follow the referential ones as shown in Figure 7.

5 Conclusion

In this paper, we discussed the cooperative control of two flexible manipulators handling an object in 3D space. Kinematics and statics of the cooperating flexible manipulators are formulated by considering the task vectors. To handle the object, hybrid position/force control based upon the kinematics and statics is established. Moreover, vibration suppression control based upon the dynamics of the manipulators is added. The stability of the system is not proved theoretically, and the effect of the position and force control on the vibrations are not analyzed. However, the experimental results illustrate that the proposed control scheme is effective for handling a rigid object practically. The future work will be directed to theoretical analysis of the vibration and the stability.

References

[1] A. Konno and M. Uchiyama, "Modeling of Flexible Manipulator Dynamics Based upon Holzer's Model," *Proc. 1996 IEEE/RSJ Int. Conf. on Intelligent Robots and Systems*, Osaka, pp. 223–229, 1996.

[2] M. Uchiyama and A. Konno, "Computed Acceleration Control for Vibration Suppression of Flexible Robot Manipulators," *Proc. Fifth Int. Conf. on Advanced Robotics*, Pisa, pp. 126–131, 1991.

[3] B. C. Chiou and M. Shahinpoor, "Dynamic Stability Analysis of a Two-Link Force-Controlled Flexible Manipulator," *Trans. ASME, J. of Dynamic Systems, Measurement, and Control*, vol. 112, pp. 661–666, 1990.

[4] M. M. Svinin and M. Uchiyama, "Contribution to Inverse Kinematics of Flexible Robot Arm," *JSME Int. J.*, Series C, vol. 37, no. 4, pp. 755–764, 1994.

[5] A. Konno, M. Uchiyama, Y. Kito and M. Murakami, "Vibration Controllability of Flexible Manipulators," *Proc. 1994 IEEE Int. Conf. on Robotics and Automation*, San Diego, pp. 308–314, 1994.

[6] F. Matsuno, T. Asano and Y. Sakawa, "Modeling and Quasi-Static Hybrid Position/Force Control of Constrained Planar Two-Link Flexible Manipulators," *IEEE Trans. on Robotics and Automation*, vol. 10, no. 3, pp. 287–297, 1994.

[7] J. S. Kim, K. Suzuki, A. Konno and M. Uchiyama, "Force Control of Constrained Flexible Manipulators," *Proc. 1996 IEEE Int. Conf. on Robotics and Automation*, Minneapolis, pp. 635–639, 1996.

[8] J. S. Kim, K. Suzuki, M. Yamano and M. Uchiyama, "Vibration Suppression Control of Constrained Spatial Flexible Manipulators," *Proc. 1997 IEEE Int. Conf. on Robotics and Automation*, Albuquerque, pp. 2831–2837, 1997.

[9] E. Nakano, S. Ozaki, T. Ishida and I. Kato, "Cooperational Control of the Anthropomorphous Manipulator 'MELARM'," *Proc. 4th Int. Symp. on Industrial Robots*, Tokyo, pp. 251–260, 1974.

[10] M. Uchiyama and P. Dauchez, "A Symmetric Hybrid Position/Force Control Scheme for the Coordination of Two Robots," *Proc. 1988 IEEE Int. Conf. on Robotics and Automation*, Philadelphia, pp. 350–356, 1988.

[11] K. Kosuge and H. Yoshida, "Unified Control for Dynamic Cooperative Manipulation," *Proc. 1994 IEEE/RSJ Int. Conf. on Intelligent Robots and Systems*, Munich, pp. 1042–1047, 1994.

[12] R. G. Bonitz and T. C. Hsia, "Force Decomposition in Cooperating Manipulators Using the Theory of Metric Spaces and Generalized Inverses," *Proc. 1994 IEEE Int. Conf. on Robotics and Automation*, San Diego, pp. 1521–1527, 1994.

[13] F. Matsuno and M. Hatayama, "Quasi-Static Cooperative Control of Two Two-Link Flexible Manipulators," *Proc. 1995 IEEE Int. Conf. on Robotics and Automation*, Nagoya, pp. 615–620, 1995.

[14] S. Koike, H. Shimojima and K. Yamabe, "Motion